Polyhedron 202 (2021) 115190

Contents lists available at ScienceDirect

Polyhedron

journal homepage: www.elsevier.com/locate/poly

Identification of slow magnetic relaxation and magnetocoolant capabilities of heterobimetallic lanthanide-manganese metallacrown-like compounds

Jacob C. Lutter [a], Thaddeus T. Boron III [b,*], Katelyn E. Chadwick [c], Andrew H. Davis [b], Stephen Kleinhaus [b], Jeff W. Kampf [a], Curtis M. Zaleski [c,*], Vincent L. Pecoraro [a,*]

[a] Department of Chemistry, University of Michigan, 930 N. University Ave., Ann Arbor, MI 48109-1055, USA
[b] Department of Chemistry, Slippery Rock University, 100 Central Loop, Slippery Rock, PA 16057, USA
[c] Department of Chemistry & Biochemistry, Shippensburg University, 1871 Old Main Dr., Shippensburg, PA 17257, USA

ARTICLE INFO

Article history:
Received 15 January 2021
Accepted 29 March 2021
Available online 2 April 2021

Keywords:
Single-molecule magnetism
Magnetocaloric effect
Manganese
Lanthanide
Metallacrown

ABSTRACT

Two types of 3*d*-4*f* compounds are presented, $[Dy^{III}_4Mn^{III}_4(OH)_2(O_2C_2H_3)_3(shi)_4(H_2shi)_4(Hsal)_3(DMF)_4]\cdot 3DMF$ (**Dy-1**) and $[Ln^{III}_6Mn^{III}_2Mn^{IV}_2(shi)_6(Hshi)_4(H_2shi)_2(Hsal)_4(DMF)_8]\cdot 4H_2O$ (**Ln-2**) (Ln = Dy or Gd, H_3shi = salicylhydroxamic acid, H_2sal = salicylic acid). While neither **Dy-1** and **Dy-2** demonstrated a significant barrier to magnetization relaxation, out-of-phase ac magnetic susceptibility was observed in both cases. **Gd-2** showed potential as a magnetocoolent with gravimetric entropy changes reaching a maximum of 18.89 $J\cdot kg^{-1}\cdot K^{-1}$ at 3 K and ΔH = 7 T. This value represents approximately 53% of the theoretical maximum.

1. Introduction

Molecular magnetism has been a significant research focus for the past three decades with the advent of single-molecule magnets (SMM), coordination compounds with a well-isolated magnetic ground state leading to a thermodynamic barrier to magnetic relaxation. This barrier originates from unpaired spin in the complex and the magnetoanisotropy of the compound. The first reported compound to behave as a SMM was a mixed-valent Mn^{III}_8-Mn^{IV}_4compound, also known as Mn_{12}OAc, which was first synthesized by Lis in 1980 and later identified by Gatteschi, Christou, Hendrickson, and co-workers in 1993 as a SMM [1–3]. Since this initial finding, a wide array of molecules have been reported as SMMs including 3*d*, 3*d*-4*f*, 4*f* compounds [4–9], and coordination polymers [10,11]. These compounds have been suggested for use in quantum computing, high density data storage, and spintronic applications [12,13].

In addition to SMMs, molecular magnets have demonstrated promise as magnetocoolants via the magnetocaloric effect [14,15]. What is interesting to note is that the attractive qualities for a magnetocoolant may be considered the inverse of attractive qualities for a good SMM. Compounds with degenerate magnetic ground states or easily accessible excited states and isotropic metal ions perform rather well as magnetocoolants [14]. These properties lead to the opportunity for large magnetic entropy changes (ΔS_M) with and without an applied magnetic field, which powers a Carnot-type cycle. While metal oxides such as gadolinium-gallium-garnet have current industrial capabilities [16], compounds containing iron, manganese, cobalt, and/or gadolinium have been quickly gaining attention [17–23].

Coordination compounds have seen use in both fields of molecular magnetism and in particular metallacrowns (MC), a type of metallamacrocycle, have showcased the capability for predictable molecular design offered by self-assembled supramolecular chemistry [8,9,24]. Metallacrowns are typically comprised of cyclic arrangements of transition metal ions and hydroxamic acid ligands that form a metal—N—O repeating unit analogous to the C—C—O repeat unit of crown ethers. MCs are known to encapsulate lanthanide ions, and in some cases also use ancillary ligands such as carboxylate anions to help capture the central Ln^{III} ions [25]. MCs featuring manganese, zinc, and iron have demonstrated that one may design a molecule with SMM behaviour [26–28], magnetocoolent potential [29], or tailored coordination environments to take advantage of lanthanide ion anisotropy [30,31]. In this work,

* Corresponding authors.
E-mail addresses: thaddeus.boron@sru.edu (T.T. Boron III), cmzaleski@ship.edu (C.M. Zaleski), vlpec@umich.edu (V.L. Pecoraro).

https://doi.org/10.1016/j.poly.2021.115190
0277-5387/

we report two metallacrown-like compounds comprised of manganese, salicylhydroxamic acid (H_3shi), salicylic acid (H_2sal) and either dysprosium or gadolinium, $Dy^{III}_4Mn^{III}_4(OH)_2(O_2C_2H_3)_3(shi)_4(H_2shi)_4(Hsal)_3(DMF)_4]\cdot 3DMF$ (**Dy-1**) and $[Ln^{III}_6Mn^{III}_2Mn^{IV}_2(shi)_6(Hshi)_4(H_2shi)_2(Hsal)_4(DMF)_8]\cdot 4H_2O$ (**Ln-2**) (Ln = Dy or Gd). These molecules demonstrate how one may take advantage of predictable formation of MCs to tailor a molecule for either SMM or magneto-coolant properties

2. Materials and methods

2.1. Physical methods

Elemental analyses were performed on either a Carlo Erba 1108 or a PerkinElmer 2400 elemental analyzer by Atlantic Microlabs, Inc.

2.2. Magnetic analysis

Solid samples of **Dy-1**, **Dy-2**, and **Gd-2** were ground to a homogeneous powder and suspended in eicosane within a gel capsule. The capsule was loaded into a drinking straw as a sample holder. Diamagnetic corrections were applied for the eicosane, capsule, and straw and molar diamagnetic susceptibilities were calculated from Pascal's constants.

Magnetic property analyses of **Dy-1** were collected at the University of Michigan, Department of Chemistry on a DC QD MPMS SQUID magnetometer and at the Michigan State University, Department of Physics and Astronomy on a QP MPMS AC SQUID magnetometer. Variable temperature (VT) and variable field (VF) experiments were conducted at 2000 Oe applied field between 5 and 300 K and 5 K with a varying field from 0 to 55,000 Oe, respectively. AC SQUID experiments were measured with an AC drive field of 3.5 Oe, no applied DC field, temperatures ranging from 10 to 2 K, and at frequencies ranging from 0 to 1000 Hz.

DC Magnetic property analysis of **Dy-2** were collected on a QD MPMS SQUID magnetometer at the University of Michigan, Department of Chemistry while AC magnetic property analysis was performed on a QD MPMS XL SQUID magnetometer at Université Claude Bernard Lyon 1 in Lyon, France. VT data were collected from 5 to 300 K with an applied field of 2000 Oe. VF data were collected from 0 to 55,000 Oe at a temperature of 5 K. AC susceptibility was measured from 2 to 8 K with an AC drive field of 3.5 Oe, no applied DC field, and at frequencies ranging from 10 to 1500 Hz.

Magnetic property analysis of **Gd-2** were collected on a DC QD MPMS SQUID magnetometer at the University of Michigan, Department of Chemistry. VT-VF data were collected between 2 and 20 K and 0–70,000 Oe applied field strength.

2.3. X-ray crystallography

A needle crystal of **Dy-1** (0.32x0.04x0.03 mm) was mounted on a Bruker SMART APEX CCD-based X-ray diffractometer equipped with a low temperature device and fine-focus Mo-target X-ray tube (λ = 0.71073 Å) operated at 1500 W power (50 kV, 30 mA). X-ray diffraction intensities were collected at 85(1) K with the detector placed 5.055 cm from the crystal. A total of 4095 frames were collected with a scan width of 0.5° increments of ω and 0.45° increments in φ with an exposure time of 60 s per frame. Integration of the data yielded a total of 93,898 reflections to a maximum 2θ value of 51.66°, of which 12,807 were unique and 8774 were greater than $2\sigma(I)$. The final cell constants were based on xyz centroids of 9983 reflections above $10\sigma(I)$. Analysis of the data showed negligible decay during data collection; the data were processed with SADBS and corrected for absorption. The structure was solved and refined using Bruker SHELXTL (v 6.12) software package [32].

A red plate crystal of **Gd-2** (0.08x0.05x0.01 mm) was diffracted at 150 K on a D8 goniostat equipped with a Bruker APEXII CCD detector at Beamline 11.3.1 at the Advanced Light Source (Lawrence Berkeley National Laboratory) using synchrotron radiation tuned to λ = 0.7749 Å. A series of 2-s frames measured at 0.2° increments of ω were collected to calculate a unit cell. For data collection frames were measured for a duration of 2 s for low angle data and 4 s for high angle data at 0.3° intervals of ω with a maximum 2θ value of ~ 60°. The data frames were collected using the program APEX2 and processed using the program SAINT routine within APEX2. The data were corrected for absorption and beam corrections based on the multi-scan technique as implemented in SADABS. The structure was solved and refined using Bruker SHELXTL (v 2018/3) software [32].

3. Syntheses of compounds

3.1. Materials

Salicylhydroxamic acid (H_3shi, 99%) and dysprosium(III) nitrate pentahydrate (99.9%) were purchased from Alfa Aesar. Manganese (II) acetate tetrahydrate (99+%) was purchased from Acros Organics. Sodium salicylate (99.9%) was purchased from Fisher Scientific. *N*,*N*-dimethylformamide (DMF, Certified ACS grade) was purchased from BDH Chemicals. Dysprosium(III) chloride hexahydrate and gadolinium(III) chloride hexahydrate were purchased from Sigma Aldrich. All reagents were used as received and without further purification.

$[Dy^{III}_4Mn^{III}_4(OH)_2(O_2C_2H_3)_3(shi)_4(H_2shi)_4(Hsal)_3(DMF)_4]\cdot 3DMF$ (Dy-1): Manganese(II) acetate tetrahydrate (4 mmol) was dissolved in DMF (12.5 mL) resulting in a dark orange solution. $Dy(NO_3)_3\cdot 5H_2O$ (0.5 mmol) and salicylhydroxamic acid (H_3shi; 4 mmol) were dissolved in DMF (12.5 mL) resulting in a slightly pink solution. The manganese solution was added to the Dy/H_3shi solution resulting in a dark brown solution that was subsequently stirred overnight. The solution was then gravity filtered. A dark brown precipitate was recovered and discarded, and the dark brown filtrate was slowly evaporated for 3 months. Small, brown, needle-like crystals were collected for X-ray analysis while the remaining were filtered and washed with cold DMF. The percent yield was 11% based on dysprosium(III) nitrate pentahydrate. Elemental Analysis: $Dy_4Mn_4C_{103}H_{103}N_{13}O_{47}$ [FW = 3144.76 g/mol]. found % (calculated): C = 39.65 (39.34); H = 3.58 (3.30); N = 5.35 (5.79). Unit Cell: a = 13.8909 Å, b = 17.0470 Å, c = 17.338 Å, α = 61.0230°, β = 71.249°, γ = 89.926°, V = 3341.39 Å^3.

$[Dy^{III}_6Mn^{III}_2Mn^{IV}_2(shi)_6(Hshi)_4(H_2shi)_2(Hsal)_4(DMF)_8]\cdot 4H_2O$ (Dy-2): In a beaker, manganese(II) acetate tetrahydrate (2 mmol) was dissolved in 12.5 mL DMF. In another beaker, $DyCl_3\cdot 6H_2O$ (1 mmol), H_2sal (1 mmol), and H_3shi (2 mmol) were dissolved in 13 mL DMF. When the Mn solution was red, it was added to the $DyCl_3$, H_2sal, and H_3shi solution and stirred overnight. The next day the solution was filtered, and the filtrate was allowed to evaporate slowly. Small red plates were isolated in approximately 3 weeks. The percent yield was 7.3% based on dysprosium(III) chloride hexahydrate. Elemental Analysis for $Dy_6Mn_4C_{136}H_{140}N_{20}O_{60}$ [FW = 4209.46 g/mol] found % (calculated): C = 38.81 (38.81), H = 3.30 (3.35), N = 6.65 (6.66). Unit Cell: a = 16.889 Å, b = 17.552 Å, c = 17.991 Å, α = 63.97°, β = 78.18°, γ = 70.51°, V = 4506.85 Å^3.

$[Gd^{III}_6Mn^{III}_2Mn^{IV}_2(shi)_6(Hshi)_4(H_2shi)_2(Hsal)_4(DMF)_8](DMF)_2\cdot 3H_2O$ (Gd-2): Gd-2 was synthesized using the same procedure as **Dy-2**, except $GdCl_3\cdot 6H_2O$ was used in place of $DyCl_3\cdot 6H_2O$ The percent yield was 2.1% based on gadolinium(III) chloride hexahydrate. Elemental Analysis for $Gd_6Mn_4C_{142}H_{152}N_{22}O_{61}$ [FW = 4306.12 g/mol]

found % (calculated): C = 39.63 (39.61), H = 3.46 (3.56), N = 7.12 (7.15). Unit Cell: a = 16.8643 Å, b = 17.3718 Å, c = 17.6074 Å, α = 63.622°, β = 69.783°, γ = 73.783°, V = 4287.76 Å^3.

4. Results and discussion

By careful choice of starting reagents and the stoichiometric ratios between them, two different but related compounds can be synthesized that possess metallacrown features (Fig. 1 and Table S1). The use of just $Dy(NO_3)_3$, $Mn(O_2C_2H_3)_2$, and H_3shi, leads to **Dy-1**, where some of the H_3shi is hydrolyzed to salicylate. The compound is comprised of four Dy^{III} ions and four Mn^{III} ions (total 24 + charge) that are counterbalanced by four shi^{3-}, four H_2shi^-, three $Hsal^-$, two hydroxide, and three acetate ligands (total 24- charge) (**Dy-1**, Fig. 1a). The use of $LnCl_3$, $Mn(O_2C_2H_3)_2$, H_3shi, and salicylic acid (Scheme 1) yields **Dy-2** and **Gd-2** which contains six Ln^{III} ions, two Mn^{III} ions, and two Mn^{IV} ions (total 32 + charge) that are countered by six shi^{3-}, four $Hshi^{2-}$, two H_2shi^-, and four $Hsal^-$ ligands (total 32– charge) (**Ln-2**, Fig. 1b). Beyond overall molecular charge considerations, the oxidation assignments of the metal ions are supported by average bond length values, the presence of an elongated Jahn- Teller axis on the Mn^{III} ions, typical of a high-spin $3d^4$ electron configuration, a lack of a Jahn-Teller axes on the Mn^{IV} ions, and bond valence sum (BVS) values (Tables S2 and S3).

While neither molecule is an archetypal metallacrown, with N—O bridges between all ring metal sites, both molecules can be considered MC-like with heterobimetallic Ln-Mn MC rings. **Dy-1** is positioned about an inversion center and can be considered a

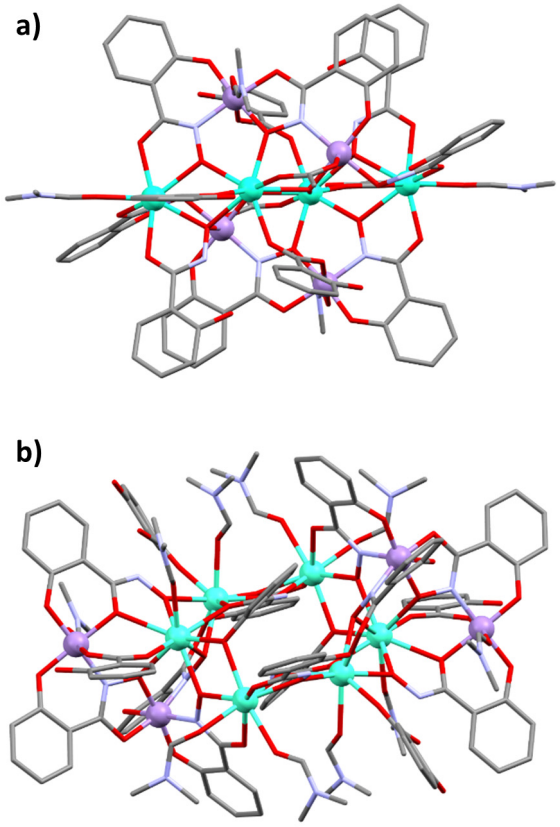

Fig. 1. Crystallographic representations of (a) **Dy-1** and (b) **Gd-2**, where hydrogen atoms, lattice solvent molecule, and disorder are removed for clarity. Teal = Dy or Gd, purple = Mn, blue = N, red = O, and grey = C. ((Colour online.))

16-MC-6 with N—O bridges between all ring metal ions except the Mn2-Dy2 connectivity which is only through an oxygen atom. For **Dy-1** a [Dy^{III}-O-Mn^{III}—N—O—Mn^{III}—N—O] repeat unit recurs twice to generate a 16-MC-6 structure that captures a $Dy^{III}_2(\mu_3\text{-}OH)_2$ core (Fig. S1). Both Dy^{III} ions (Dy1 and Dy2) of **Dy-1** are eight-coordinate and a SHAPE analysis (*SHAPE 2.1*) [33] yields the lowest Continuous Shape Measure (CShM) values for a biaugmented trigonal prism geometry (Table S4). In addition, the Dy2 ions participate in the MC ring, while the Dy1 ions comprise the $Dy_2(\mu_3\text{-}OH)_2$ core. The MC ring ions Mn1 and Mn2 are both six-coordinate with a tetragonally distorted octahedral geometry (Table S6). **Gd-2** is also centrosymmetric with a hexagonal Gd^{III} ring in the center of the molecule that is flanked on either side by one Mn^{IV} ion (Mn1) and one Mn^{III} ion (Mn2). The structure can be considered a 26-MC-10 with a [Gd^{III}-O-Gd^{III}—O—N—C—O—Mn^{III}—N—O—Mn^{IV}—N—O] repeat unit that recurs twice to generate the MC-like ring that captures two Gd^{III} ions (Fig. S2). Gd1, the captured Gd^{III} ion, is nine-coordinate with a spherical capped square antiprism geometry based on the CShM analysis, while the MC ring ions Gd2 and Gd3 are eight-coordinate with triangular dodecahedron and biaugmented trigonal prism geometry, respectively (Tables S4 and S5). Both MC rings ions Mn1 and Mn2 are six-coordinate with octahedral geometry (Table S6); however, Mn2 possesses a tetragonal distortion as it is a Mn^{III} ion with a high spin $3d^4$ electron configuration and Mn1 does not possess a distortion as it is a Mn^{IV} ion. Both **Dy-1** and **Gd-2** are similar to two other MC-like molecules we have previously reported: $Ho^{III}_4Mn^{III}_6$ and $Dy^{III}_6Mn^{III}_4Mn^{IV}_2$ [34,35]. The $Ho^{III}_4Mn^{III}_6$ structure can be considered a 22-MC-8 with a heterobimetallic Ho^{III}_2/Mn^{III}_6 MC ring that captures a $Ho^{III}_2(\mu_3\text{-}OH)_2$ core, similar to **Dy-1**. The $Dy^{III}_6Mn^{III}_4$-Mn^{IV}_2 structure consists of a hexagonal ring of Dy^{III} ions that is flanked on either side by a $Mn^{III}_2Mn^{IV}$ trimer, similar to **Gd-2**, and can be considered a 28-MC-10 with four Dy^{III} and six $Mn^{III/IV}$ ions in the MC ring and two captured Dy^{III} ions.

DC and AC magnetic susceptibility measurements were determined for both dysprosium compounds **Dy-1** and **Dy-2** as the high intrinsic spin values and strong magnetoanisotropy associated with Mn^{3+} and Dy^{3+} ions could lead to slow relaxation of the magnetization. Variable temperature DC magnetic susceptibility was measured from 5 to 300 K for both **Dy-1** and **Dy-2** (Fig. S3). The χ_MT value at 300 K for **Dy-1** (50.00 $cm^3{\cdot}mol^{-1}{\cdot}K$) is less than that expected for the isolated ions (68.68 $cm^3{\cdot}mol^{-1}{\cdot}K$) [35] and the χ_MT value reaches a minimum at 5 K (36.94 $cm^3{\cdot}mol^{-1}{\cdot}K$). For **Dy-2** the χ_MT value at 300 K (81.13 $cm^3{\cdot}mol^{-1}{\cdot}K$) is less than that expected for the isolated ions (94.77 $cm^3{\cdot}mol^{-1}{\cdot}K$) [36] and the χ_MT value reaches a minimum at 5 K (68.78 $cm^3{\cdot}mol^{-1}{\cdot}K$). The suppression of magnetic susceptibility at 300 K and the decrease in χ_MT at lower temperatures are likely due to antiferromagnetic coupling of metal ions in the compounds and long-range intermolecular exchange interactions. Variable field DC magnetization were also measured for **Dy-1** and **Dy-2** (Fig. S4) and neither compound shows saturation up to 7 Tesla.

Variable temperature AC susceptibility was also measured for both **Dy-1** and **Dy-2** from 2 to 10 K and 2–8 K, respectively (Fig. 2). **Dy-1** did display out-of-phase magnetic susceptibility with frequency dependence in this temperature range; however, the signal did not appear to reach a maximum above 2 K. **Dy-2** did not show peak maxima within the observed temperature range either. However, based on the larger deviation in curvature of the in-phase susceptibility of **Dy-2** as a function of frequency, the frequency dependence is more obvious between 2 and 5 K when compared to **Dy-1**. The presence of out-of-phase susceptibility for both compounds suggests there is a barrier to magnetic relaxation albeit the barrier is likely small. Cole-Cole plots (Fig. S5) of both **Dy-1** and **Dy-2** are neither semi-circular nor symmetrical, which is likely due to complex and numerous interactions between the metal centers

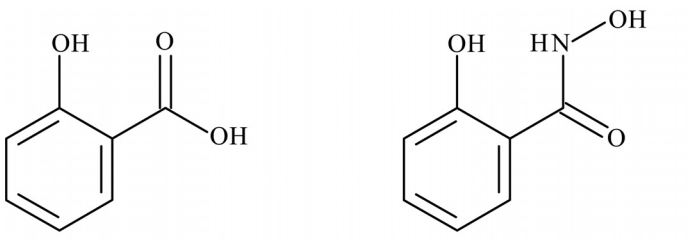

Salicylic acid (H_2sal) Salicylhydroxamic acid (H_3shi)

Scheme 1. Parent Ligands of **Ln-1** and **Ln-2**.

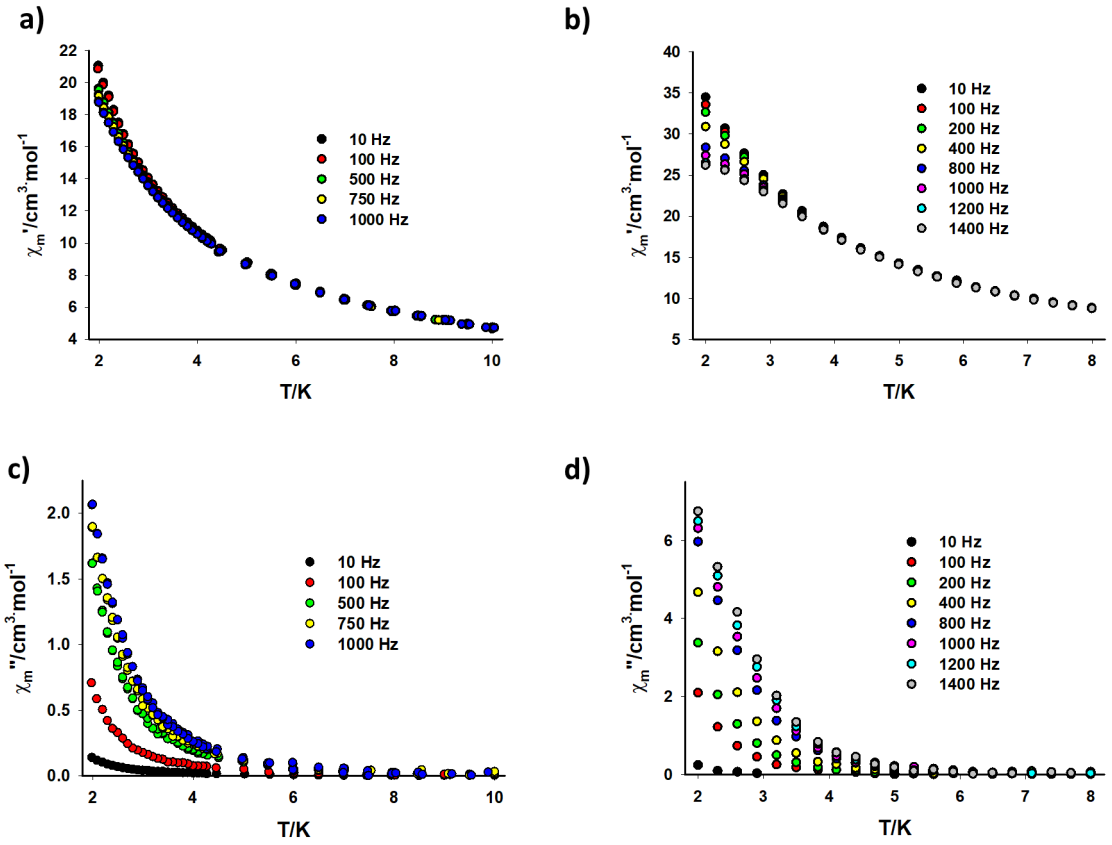

Fig. 2. AC susceptibility for **Dy-1** both (a) in-phase and (c) out-of-phase, and **Dy-2** for both (b) in-phase and (d) out-of-phase measurements.

of the molecules and the lack of a well-isolated magnetic ground state.

The lack of a well-isolated ground state may not be ideal for SMM behavior; however, for magnetocoolants such a quality is considered attractive. Since isotropic ions are often featured in magnetocoolants, we chose to examine **Gd-2** as Mn^{4+} is more isotropic than Mn^{3+} and a greater amount of Gd^{3+} ions is possible in this structural motif compared to a potential **Gd-1**. Isothermal DC magnetization experiments ranging from 2 to 20 K were performed (Fig. 3a) and the gravimetric magnetic entropy change ($-\Delta S_{Mg}$) was calculated according to the Maxwell relation: [14]

$$-\Delta S_{Mg} = \int_{H_o}^{H_f} \left(\frac{\delta M_g}{\delta T}\right) dH \quad (1)$$

where H is field strength, M_g is the gravimetric magnetization, and T is temperature. (Fig. 3b). **Gd-2** demonstrated a maximum $-\Delta S_{Mg}$ of 18.89 $J{\cdot}kg^{-1}{\cdot}K^{-1}$ at 4 K with a ΔH of 7 Tesla. This value is about 53% of the theoretical maximum value of 35.66 $J{\cdot}kg^{-1}{\cdot}K^{-1}$ obtained from:

$$-\Delta S_M = R\sum n_i ln(2S_i + 1) \quad (2)$$

where R is the ideal gas constant, and n_i and S_i are the number and spin of each unique metal center, assuming non-interacting spin between the metal centers. In addition, the generally slow increase in magnetization as a function of applied field implies that **Gd-2** does have low-lying excited states near the ground state, which are indicative of a good MCE candidate. These observations are consistent with the small barrier to relaxation observed in **Dy-**

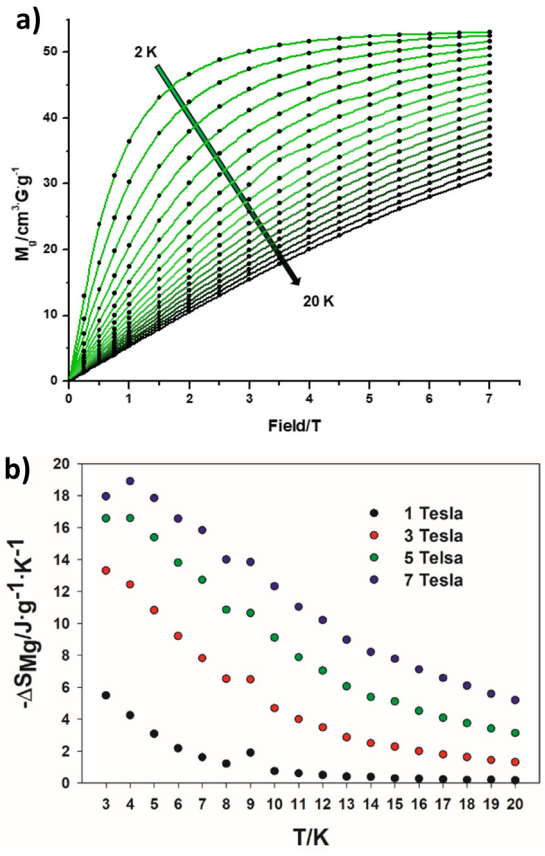

Fig. 3. (a) Isothermal DC magnetization curves for **Gd-2** from 2 to 20 K and (b) isothermal entropic change (-ΔS_{Mg}) calculated from Eq. (1) at various ΔH.

2. Comparison of **Gd-2** to other reported Gd-Mn cluster complexes is shown in Table 1 [37–40]. In terms of -ΔS_{Mg} values, **Gd-2** is comparable to calixarene complexes and calculated values for small cluster compounds, but phosphonate cage complexes reported by Winpenny and coworkers had higher values, likely due to the fact that these complexes contain isotropic high-spin d^5 Mn^{2+} ions rather than Mn^{3+} and Mn^{4+} ions. However, in terms of the percentage of ideal magnetic entropy, **Gd-2** is only outperformed by two of the compounds listed in Table 1.

5. Conclusions

Two heterobimetallic 3*d*-4*f* lanthanide-manganese compounds (**Dy-1** and **Dy-2**) were investigated for slow magnetic relaxation and did indeed display observable out-of-phase susceptibility consistent with the presence of a barrier to magnetic relaxation. However, no peak maxima were observed for either compound, suggesting that these barriers are small and it is likely these molecules do not possess well-isolated ground states. Thus, **Gd-2** was studied for potential as a magnetocoolant material and subsequently the gravimetric magnetic entropy change (-ΔS_{Mg}) was determined to be 18.89 J·kg^{-1}K^{-1} at 7 T applied field. While **Dy-1** and **Dy-2** were not ideal as SMMs, **Gd-2** demonstrated surprising potential as a magnetocoolant despite the relatively large amount of diamagnetic atoms in the compound compared to other Gd-Mn compounds. These results demonstrate that self-assembled MCs and related molecules can be tailored to a particular application by careful selection of starting components. In addition, the investigation of both SMM and MCE properties can give valuable information for potential applications of magnetic materials.

Declaration of Competing Interest

The authors declare that they have no known competing financial interests or personal relationships that could have appeared to influence the work reported in this paper.

Acknowledgments

Crystallographic information in CIF format are available free of charge from the CCDC website (www.ccdc.cam.ac.uk) using deposition numbers CSD 2056275 and 2056276. Crystallographic data for **Gd-2** were collected through the SCrALS (Service Crystallography at Advanced Light Source) program at the Small-Crystal Crystallography Beamline 11.3.1 at the Advanced Light Source (ALS), Lawrence Berkeley National Laboratory. The ALS is supported by the U.S. Department of Energy, Office of Energy Sciences Materials Sciences Division, under contract DE-AC02-05CH11231.

JCL and VLP would like to thank the National Science Foundation for funding (CHE-1664964). JWK recognizes funding from the National Science Foundation (CHE-0840456). CMZ acknowledges funding from the Shippensburg University CFEST Teaching and Research Excellence Award.

CMZ would like to thank Matthias Zeller at Purdue University for useful conversations regarding the crystal structure of **Dy-1**. TTB would like to thank Talal Mallah at Université Paris Sud 11 and Dominique Luneau for useful conversations regarding the magnetic data. TTB would like to thank Reza Loloee at Michigan State University and Dominique Luneau at Université Claude Bernard Lyon 1 for access to their magnetometers.

Appendix A. Supplementary data

Supplementary data to this article can be found online at https://doi.org/10.1016/j.poly.2021.115190.

Table 1
Comparison of MCE behaviour of Gd and Mn containing complexes.

Compound Description	-ΔS_{Mg} (J·kg^{-1}·K^{-1})	Theoretical Maximum -ΔS_M Value (J·kg^{-1}·K^{-1})	Percentage (%) of Ideal Magnetic Entropy	Conditions	Ref
$Gd^{III}_4Mn^{III}_4$ calix[4]arene	19.0	37.1	51	4 K, 7 T	38, 40
$Gd^{III}_9Mn^{II}_9$ phosphonate cage	28.0	57.0	49	3 K, 7 T	39
$Gd^{III}_6Mn^{II}_4$ phosphonate cage	33.7	41.8	81	3 K, 7 T	39
$Gd^{III}Mn^{III}_2$[a]	13.5	45.79	29	3 K, 9 T	37
$Gd^{III}Mn^{III}_2$ [a]	20.39	37.91	54	3 K, 9 T	37
$Gd^{III}Mn^{III}_2$[a]	19.73	36.64	54	3 K, 9 T	37
$Gd^{III}Mn^{III}_2$[a]	31.75	38.14	83	3 K, 9 T	37
$Gd^{III}Mn^{III}_2$[a]	19.0	44.48	43	3 K, 9 T	37
$Gd^{III}_6Mn^{III}_2Mn^{IV}_2$	18.89	35.66	53	4 K, 7 T	This Work

[a] Based on computational magnetic coupling values.

References

[1] T. Lis, Preparation, Structure, and Magnetic Properties of a Dodecanuclear Mixed-Valence Manganese Carboxylate, Acta Crystallogr. B 36 (9) (1980) 2042–2046, https://doi.org/10.1107/S0567740880007893l0.1107/S0567740880007893/a19066_35276sup1.pdf.

[2] R. Sessoli, H.L. Tsai, A.R. Schake, S. Wang, J.B. Vincent, K. Folting, D. Gatteschi, G. Christou, D.N. Hendrickson, High-Spin Molecules: $[Mn_{12}O_{12}(O_2CR)_{16}(H_2O)_4]$, J. Am. Chem. Soc. 115 (5) (1993) 1804–1816, https://doi.org/10.1021/ja00058a027.

[3] N.E. Chakov, S.C. Lee, A.G. Harter, P.L. Kuhns, A.P. Reyes, S.O. Hill, N.S. Dalal, W. Wernsdorfer, K.A. Abboud, G. Christou, The Properties of the $[Mn_{12}O_{12}(O_2CR)_{16}(H_2O)_4]$ Single-Molecule Magnets in Truly Axial Symmetry: $[Mn_{12}O_{12}(O_2CCH_2Br)_{16}(H_2O)_4]\cdot 4CH_2Cl_2$, J. Am. Chem. Soc. 128 (21) (2006) 6975–6989, https://doi.org/10.1021/ja060796n.

[4] P. Zhang, Y.N. Guo, J. Tang, Recent Advances in Dysprosium-Based Single Molecule Magnets: Structural Overview and Synthetic Strategies, Coord. Chem. Rev. 257 (11–12) (2013) 1728–1763, https://doi.org/10.1016/j.ccr.2013.01.012.

[5] S. Demir, I.-R.-R. Jeon, J.R. Long, T.D. Harris, Radical Ligand-Containing Single-Molecule Magnets, Coord. Chem. Rev. 289–290 (1) (2014) 1–28, https://doi.org/10.1016/j.ccr.2014.10.012.

[6] H.L.C.C. Feltham, S. Brooker, Review of Purely 4f and Mixed-Metal Nd-4f Single-Molecule Magnets Containing Only One Lanthanide Ion, Coord. Chem. Rev. 276 (2014) 1–33, https://doi.org/10.1016/j.ccr.2014.05.011.

[7] S. Lee, T. Ogawa, Molecular Design for Single-Molecule Magnetism of Lanthanide Complexes, Chem. Lett. 46 (1) (2017) 10–18, https://doi.org/10.1246/cl.160800.

[8] C.Y. Chow, E.R. Trivedi, V. Pecoraro, C.M. Zaleski, Heterometallic Mixed 3d–4f Metallacrowns: Structural Versatility, Luminescence, and Molecular Magnetism, Comments Inorg. Chem. 35 (4) (2015) 214–253, https://doi.org/10.1080/02603594.2014.981811.

[9] Lutter, J. C.; Zaleski, C. M.; Pecoraro, V. L. Metallacrowns: Supramolecular Constructs With Potential in Extended Solids, Solution-State Dynamics, Molecular Magnetism, and Imaging. In Advances in Inorganic Chemistry, Vol 71 Supramolecular Chemistry; Eldik, R. van, Puchta, R., Eds.; Elsevier, 2018; pp 177–246. https://doi.org/10.1016/bs.adioch.2017.11.007.

[10] S. Biswas, H.S. Jena, S. Sanda, S. Konar, Proton-Conducting Magnetic Coordination Polymers, Chem. - A Eur. J. 21 (39) (2015) 13793–13801, https://doi.org/10.1002/chem.201501526.

[11] L. Croitor, E.B. Coropceanu, O. Petuhov, K.W. Krämer, S.G. Baca, S.-X. Liu, S. Decurtins, M.S. Fonari, A One-Dimensional Coordination Polymer Based on Cu_3-Oximato Metallacrowns Bridged by Benzene-1,4-Dicarboxylato Ligands: Structure and Magnetic Properties, Dalton Trans. 44 (17) (2015) 7896–7902, https://doi.org/10.1039/c5dt00533g.

[12] R.P. Winpenny, Quantum Information Processing Using Molecular Nanomagnets as Qubits, Angew. Chemie - Int. Ed. 47 (42) (2008) 7992–7994, https://doi.org/10.1002/anie.v47:4210.1002/anie.200802742.

[13] L. Bogani, W. Wernsdorfer, Molecular Spintronics Using Single-Molecule Magnets, Nat. Mater. 7 (3) (2008) 179–186, https://doi.org/10.1038/nmat2133.

[14] J. Romero Gómez, R. Ferreiro Garcia, D.M.A. Catoira, M. Romero Gómez, Magnetocaloric Effect: A Review of the Thermodynamic Cycles in Magnetic Refrigeration, Renew. Sustain. Energy Rev. 17 (2013) 74–82, https://doi.org/10.1016/j.rser.2012.09.027.

[15] R. Sessoli, Chilling with Magnetic Molecules, Angew. Chemie - Int. Ed. 51 (1) (2012) 43–45, https://doi.org/10.1002/anie.201104448.

[16] A.C. Sackville Hamilton, G.I. Lampronti, S.E. Rowley, S.E. Dutton, Enhancement of the Magnetocaloric Effect Driven by Changes in the Crystal Structure of Al-Doped GGG, $Gd_3Ga_{5-x}Al_xO_{12}$ ($0 \leq x \leq 5$), J. Phys. Condens. Matter 26 (11) (2014) 116001, https://doi.org/10.1088/0953-8984/26/11/116001.

[17] R. Shaw, R.H. Laye, L.F. Jones, D.M. Low, C. Talbot-Eeckelaers, Q. Wei, C.J. Milios, S. Teat, M. Helliwell, J. Raftery, M. Evangelisti, M. Affronte, D. Collison, E.K. Brechin, E.J.L. McInnes, 1,2,3-Triazolate-Bridged Tetradecametallic Transition Metal Clusters $[M_{14}(L)_6O_6(OMe)_{18}X_6]$ (M = Fe^{III}, Cr^{III} and VIII/IV) and Related Compounds: Ground-State Spins Ranging from S = 0 to S = 25 and Spin-Enhanced Magnetocaloric Effect, Inorg. Chem. 46 (12) (2007) 4968–4978, https://doi.org/10.1021/ic070320k.

[18] A. Adhikary, H.S. Jena, S. Konar, A Family of Fe 3+ Based Double-Stranded Helicates Showing a Magnetocaloric Effect, and Rhodamine B Dye and DNA Binding Activities, Dalt. Trans. 44 (35) (2015) 15531–15543, https://doi.org/10.1039/C5DT01569C.

[19] K. Wang, H.-H. Zou, Z.-L. Chen, Z. Zhang, W.-Y. Sun, F.-P. Liang, A Series of 3D Metal Organic Frameworks Based on [24-MC-6] Metallacrown Clusters: Structure, Magnetic and Luminescence Properties, Dalt. Trans. 43 (34) (2014) 12989, https://doi.org/10.1039/C4DT01593B.

[20] X. Tang, Q. Zhong, J. Xu, H. Li, S. Xu, X. Cui, B. Wei, Y. Ma, R. Yuan, $Co(II)_4Gd(III)_6$ Phosphonate Grid and Cage as Molecular Refrigerants, Inorganica Chim. Acta 442 (2016) 195–199, https://doi.org/10.1016/j.ica.2015.12.013.

[21] C.-M. Liu, D.-Q. Zhang, D.-B. Zhu, Heptanuclear 3d–4f Cluster Complexes with a Coaxial Double-Screw-Propeller Topology and Diverse Magnetic Properties, Dalt. Trans. 39 (2010) 11325–11328, https://doi.org/10.1039/c0dt01189d.

[22] P. Richardson, D.I. Alexandropoulos, L. Cunha-Silva, G. Lorusso, M. Evangelisti, J. Tang, T.C. Stamatatos, 'All Three-in-One': Ferromagnetic Interactions, Single-Molecule Magnetism and Magnetocaloric Properties in a New Family of $[Cu_4Ln]$ (Ln^{III} = Gd, Tb, Dy) Clusters, Inorg. Chem. Front. 2 (10) (2015) 945–948, https://doi.org/10.1039/C5QI00146C.

[23] G. Lorusso, O. Roubeau, M. Evangelisti, Rotating Magnetocaloric Effect in an Anisotropic Molecular Dimer, Angew. Chemie - Int. Ed. 55 (10) (2016) 3360–3363, https://doi.org/10.1002/anie.201510468.

[24] G. Mezei, C.M. Zaleski, V.L. Pecoraro, Structural and Functional Evolutions of Metallacrowns, Chem. Rev. 107 (11) (2007) 4933–5003, https://doi.org/10.1021/cr078200h.

[25] M.R. Azar, T.T. Boron, J.C. Lutter, C.I. Daly, K.A. Zegalia, R. Nimthong, G.M. Ferrence, M. Zeller, J.W. Kampf, V.L. Pecoraro, C.M. Zaleski, Controllable Formation of Heterotrimetallic Coordination Compounds: Systematically Incorporating Lanthanide and Alkali Metal Ions into the Manganese 12-Metallacrown-4 Framework, Inorg. Chem. 53 (3) (2014) 1729–1742, https://doi.org/10.1021/ic402865p.

[26] C.M. Zaleski, S. Tricard, E.C. Depperman, W. Wernsdorfer, T. Mallah, M.L. Kirk, V.L. Pecoraro, Single Molecule Magnet Behavior of a Pentanuclear Mn-Based Metallacrown Complex: Solid State and Solution Magnetic Studies, Inorg. Chem. 50 (22) (2011) 11348–11352, https://doi.org/10.1021/ic2008792.

[27] T.T. Boron, J.C. Lutter, C.I. Daly, C.Y. Chow, A.H. Davis, A. Nimthong-Roldán, M. Zeller, J.W. Kampf, C.M. Zaleski, V.L. Pecoraro, The Nature of the Bridging Anion Controls the Single-Molecule Magnetic Properties of DyX_4M 12-Metallacrown-4 Complexes, Inorg. Chem. 55 (20) (2016) 10597–10607, https://doi.org/10.1021/acs.inorgchem.6b01832.

[28] T.T. Boron, J.W. Kampf, V.L. Pecoraro, A Mixed 3d–4f 14-Metallacrown-5 Complex That Displays Slow Magnetic Relaxation through Geometric Control of Magnetoanisotropy, Inorg. Chem. 49 (20) (2010) 9104–9106, https://doi.org/10.1021/ic101121d.

[29] C.Y. Chow, R. Guillot, E. Rivière, J.W. Kampf, T. Mallah, V.L. Pecoraro, Synthesis and Magnetic Characterization of Fe(III)-Based 9-Metallacrown-3 Complexes Which Exhibit Magnetorefrigerant Properties, Inorg. Chem. 55 (20) (2016) 10238–10247, https://doi.org/10.1021/acs.inorgchem.6b01404.

[30] C.Y. Chow, H. Bolvin, V.E. Campbell, R. Guillot, J.W. Kampf, W. Wernsdorfer, F. Gendron, J. Autschbach, V.L. Pecoraro, T. Mallah, Assessing the Exchange Coupling in Binuclear Lanthanide(<scp>iii</Scp>) Complexes and the Slow Relaxation of the Magnetization in the Antiferromagnetically Coupled Dy_2 Derivative, Chem. Sci. 6 (7) (2015) 4148–4159, https://doi.org/10.1039/C5SC01029B.

[31] J.C. Lutter, S.V. Eliseeva, J.W. Kampf, S. Petoud, V.L. Pecoraro, A Unique Ln III [3.3.1]Ga III Metallacryptate Series That Possesses Properties of Slow Magnetic Relaxation and Visible/Near-Infrared Luminescence, Chem. - A Eur. J. 24 (42) (2018) 10773–10783, https://doi.org/10.1002/chem.201801355.

[32] G.M. Sheldrick, Crystal Structure Refinement with SHELXL, Acta Crystallogr. Sect. C Struct. Chem. 71 (1) (2015) 3–8, https://doi.org/10.1107/S2053229614024218.

[33] Llunell M, Casanova D, Cirera J, Alemany P, Alvarez S (2013) SHAPE, version 2.1; Barcelona, Spain.

[34] C.M. Zaleski, J.W. Kampf, T. Mallah, M.L. Kirk, V.L. Pecoraro, Assessing the Slow Magnetic Relaxation Behavior of $Ln_4^{III}Mn_6^{III}$ Metallacrowns, Inorg. Chem. 46 (6) (2007) 1954–1956, https://doi.org/10.1021/ic062164810.1021/ic0621648.s00110.1021/ic0621648.s002.

[35] C.M. Zaleski, E.C. Depperman, J.W. Kampf, M.L. Kirk, V.L. Pecoraro, Single-Molecule Magnets and Chains of Single-Molecule Magnets. 45 (25) (2006) 10022–10024.

[36] C. Benelli, D. Gatteschi, Magnetism of Lanthanides in Molecular Materials with Transition-Metal Ions and Organic Radicals, Chem. Rev. 102 (6) (2002) 2369–2388, https://doi.org/10.1021/cr010303r.

[37] T. Rajeshkumar, R. Jose, P.R. Remya, G. Rajaraman, Theoretical Studies on Trinuclear MnIII2GdIII and Tetranuclear MnIII2GdIII2 Clusters: Magnetic Exchange, Mechanism of Magnetic Coupling, Magnetocaloric Effect, and Magneto-Structural Correlations, Inorg. Chem. 58 (18) (2019) 11927–11940, https://doi.org/10.1021/acs.inorgchem.9b0150310.1021/acs.inorgchem.9b01503.s001.

[38] G. Karotsis, S. Kennedy, S.J. Teat, C.M. Beavers, D.A. Fowler, J.J. Morales, M. Evangelisti, S.J. Dalgarno, E.K. Brechin, Calix[4]Arene Clusters as Enhanced Magnetic Coolers and Molecular Magnets, J. Am. Chem. Soc. 132 (37) (2010) 12983–12990, https://doi.org/10.1021/ja104848m.

[39] Y.-Z. Zheng, E.M. Pineda, M. Helliwell, R.E.P. Winpenny, Mn^{II}-Gd^{III} Phosphonate Cages with a Large Magnetocaloric Effect, Chem. - A Eur. J. 18 (14) (2012) 4161–4165, https://doi.org/10.1002/chem.v18.1410.1002/chem.201200152.

[40] G. Karotsis, M. Evangelisti, S. Dalgarno, E. Brechin, A Calix[4]Arene 3d/4f Magnetic Cooler, Angew. Chemie - Int. Ed. 48 (52) (2009) 9928–9931, https://doi.org/10.1002/anie.v48:5210.1002/anie.200905012.